

Gadolinium Retention in the Brain of Mother and Pup Mouse: Effect of Pregnancy and Repeated Administration of Gadolinium-Based Contrast Agents

Xiang Yao, PhD, Haoran Zhang, PhD, Dafa Shi, PhD, Yanfei Li, PhD, Qiu Guo, MD, Ziyang Yu, PhD, Siyuan Wang, MD, and Ke Ren, PhD^{*} 

Background: The association of repeated administration of gadolinium-based contrast agents (GBCAs) with the gadolinium (Gd) retention in the brains of mother and fetus remains unclear.

Purpose: To investigate the effects of pregnancy and repeated administration of GBCAs on Gd retention in the brains of mother and pup mice.

Study type: Cross-sectional cohort toxicity study.

Animal Model: From gestational days 16–19, pregnant ($n = 48$) BALB/c mice.

Field Strength: A 9.4 T and fast spin echo sequence.

Assessment: Half of the mother mice ($n = 24$) were killed at postnatal day 1 (P1) for inductively coupled plasma mass spectrometry (ICP-MS) and transmission electron microscopy (TEM). Besides the ICP-MS and TEM, four pups were randomly selected from each mother and killed at P1 for ultraperformance liquid chromatography mass spectrometry (UPLC-MS) and Nissl staining.

Statistical Tests: One-way analysis of variance and unpaired t -test.

Results: In the group of gadodiamide, retention of Gd in the brains of pregnant mice was significantly lower than that of nonpregnant mice in the area of the deep cerebellar nuclei (DCN) (10.35 ± 2.16 nmol/g vs. 18.74 ± 3.65 nmol/g). Retention of Gd in the DCN of pups whose mothers were administered gadoterate meglumine was significantly lower than that of pups whose mothers were administered gadodiamide (0.21 ± 0.09 nmol/g vs. 6.15 ± 3.21 nmol/g) at P1. In mice treated with gadodiamide, most of the retained Gd in the brain tissue was insoluble ($19.5\% \pm 9.5\%$ of the recovered amount corresponded to the intact complex in the DCN).

Data Conclusion: In different brain areas of the mother and pup mice, the retention of Gd after gadoterate meglumine administration was lower than that of gadodiamide and gadopentetate dimeglumine administration, and almost all the detected Gd in pups' brains was intact soluble GBCAs.

Evidence Level: 1

Technical Efficacy: Stage 2

J. MAGN. RESON. IMAGING 2022;56:835–845.

The use of gadolinium-based contrast agents (GBCAs) during pregnancy is a controversial issue due to their ability to cross the placental barrier.¹ However, the long-term effects of GBCAs exposure in utero are unclear. The latest version of the American College of Radiology Manual on Contrast Media recommends that, for pregnant or potentially pregnant patients, “GBCAs should be used only when the use of GBCAs is

considered critical and the potential benefits justify the potential unknown risk to the fetus.”² Similarly, the guidelines of the Contrast Medium Safety Committee of the European Society of Urogenital Radiology distinguish between different GBCAs, suggesting that “when there are very strong signs of MR enhancement, the smallest possible dose of one of the most stable gadolinium contrast agents can be provided to pregnant females.”³

View this article online at wileyonlinelibrary.com. DOI: 10.1002/jmri.28086

Received Oct 27, 2021, Accepted for publication Jan 18, 2022.

*Address reprint requests to: K.R., Department of Radiology, Xiang'an Hospital of Xiamen University, 2000 Xiang'an East Street, Xiamen 361000, China.
E-mail: 643034295@qq.com

From the Department of Radiology, Xiang'an Hospital of Xiamen University, School of Medicine, Xiamen University, Xiamen, China

This is an open access article under the terms of the [Creative Commons Attribution-NonCommercial-NoDerivs](https://creativecommons.org/licenses/by-nc-nd/4.0/) License, which permits use and distribution in any medium, provided the original work is properly cited, the use is non-commercial and no modifications or adaptations are made.

In recent years, adverse reactions related to the use of GBCAs have drawn substantial attention. Human and animal model studies have revealed that repeated intravenous injections of GBCAs resulted in increased signal intensities in the deep cerebellar nucleus (DCN) and globus pallidus on unenhanced T₁-weighted magnetic resonance (MR) images.^{4–7} The toxicity of GBCAs is widely recognized and occurs after the dissociation of gadolinium (Gd) ions from chelate. However, the clinical importance of this deposition has not been established. The amount and chemical form of retained Gd entering the brain parenchyma is determined by the thermodynamic and kinetic stability of GBCAs. Specifically, the chemical form is strongly influenced by the composition of the medium, the elution rate through the lymphatic system, and the overall chemical degradation of GBCAs, among other factors.^{8,9}

This study aimed to investigate GBCAs types on the retention of Gd in the brains of mother and pup mice after maternal administration. In addition, we also quantified the amount of intact Gd complexes and insoluble Gd-containing species recovered from the brains.

Methods

Animals and Study Design

All studies were approved by the Animal Ethics Committee of our institution. Forty-eight pregnant BALB/c mice (5 weeks old; 15 embryonic days [E15]) and 24 nonpregnant female mice (5 weeks old) were purchased from Xiamen University Laboratory Animal Center (Xiamen, China).

Gadodiamide (linear and nonionic GBCAs, Omniscan, 500 mmol Gd/L; GE Healthcare), gadopentetate dimeglumine (linear and ionic GBCAs, Magnevist, 500 mmol Gd/L; Bayer Healthcare), gadoterate meglumine (macrocylic and ionic GBCAs, Dotarem, 500 mmol Gd/L; Guerbet), and saline were used in this study. Forty-eight pregnant mice were randomly divided into four groups: gadodiamide group ($n = 12$), gadopentetate dimeglumine group ($n = 12$), gadoterate meglumine group ($n = 12$), and saline group ($n = 12$). GBCAs were injected via the tail vein for 4 consecutive days (E16–E19) at a dose of 2.0 mmol/kg. Twenty-four nonpregnant mice in the control groups were also randomly divided into four groups: gadodiamide group ($n = 6$), gadopentetate dimeglumine group ($n = 6$), gadoterate meglumine group ($n = 6$), and saline group ($n = 6$). These mice were also received GBCAs and saline injections for 4 consecutive days. The saline group received 100 μ L saline for 4 consecutive days to estimate the limit of detection (LOD) and limit of quantification (LOQ).

Half of the mother mice ($n = 24$) were killed at postnatal day 1 (P1) for inductively coupled plasma mass spectrometry (ICP-MS) and transmission electron microscopy (TEM). Besides the ICP-MS and TEM, four pups were randomly selected from each mother and killed at P1 for

ultraperformance liquid chromatography mass spectrometry (UPLC-MS) and Nissl staining. The pups were fed their mothers' ($n = 24$) milk and kept in the same cages for 21 days after delivery at E19. On day 21 after birth (P21), the pups were separated from their mothers and fed standard food and water for the next 7 days. Three pups were randomly selected from each mother and killed at postnatal day 28 (P28) for ICP-MS, Nissl staining, and UPLC-MS analysis. Nonpregnant mice ($n = 24$) in the control group were treated with the same method, they were killed at P1 for ICP-MS and TEM. A schematic of the study groups including all regimens is presented in Fig. 1.

MR Imaging and Analysis

The mice were anesthetized (1.5% isoflurane) and stationed on a mechanical ventilator. During the administration period, MRI was performed after 4 days of continuous administration to ensure a 72 hours clearance period for Gd. Body core temperature was maintained at $37.0 \text{ }^{\circ}\text{C} \pm 0.5 \text{ }^{\circ}\text{C}$ using a heated circulating water pad. The mice were placed in a stereotactic stent for MRI. MRI experiments were performed on a horizontal bore 9.4 T scanner operating on a Bruker AVANCE platform (Bruker 9.4 T Biospec). T₁-weighted MRI was performed with a fast spin echo sequence on the brain of pregnant and nonpregnant mice (field of view [FOV] = 40×40 mm, bandwidth = 348.77 kHz, matrix size = 256×256 , slice thickness = 1.0 mm, echo time [TE] = 8.5 msec, repetition time [TR] = 1366.9 msec, and number of excitations [NEX] = 15), the brain of pup mice (FOV = 20×20 mm, bandwidth = 348.77 kHz, matrix size = 256×256 , slice thickness = 0.5 mm, TE = 8.5 msec, TR = 1000 msec, and NEX = 10). T₂-weighted MRI was performed on the abdominal of pregnant mice (FOV = 80×80 mm, bandwidth = 348.77 kHz, matrix size = 256×256 , slice thickness = 1.0 mm, TE = 33 msec, TR = 3053 msec, and NEX = 28).^{10,11}

All images were analyzed under blind and random conditions. According to the anatomy of the mouse brain, regions of interest (ROIs) were located in the bilateral DCN and cerebellum (Fig. 2a,b). All sections were drawn by XY with 7 years of experience. Each ROI of delineation was validated by a second professional radiologist (KR) with over 30 years of experience. The DCN T₁ signal intensity was quantitatively evaluated. The signal intensity ratio was calculated as follows^{6,12}:

$$\text{Ratio} = \frac{\text{Signal intensity (DCN)}}{\text{Signal intensity (Cerebellum)}}$$

ICP-MS Analysis

Gd content in the brain homogenate was determined by ICP-MS analysis. The samples were prepared for ICP-MS analysis as follows: 1) 1 mL of concentrated nitric acid (70%) was added to each lyophilized homogenate and the sample

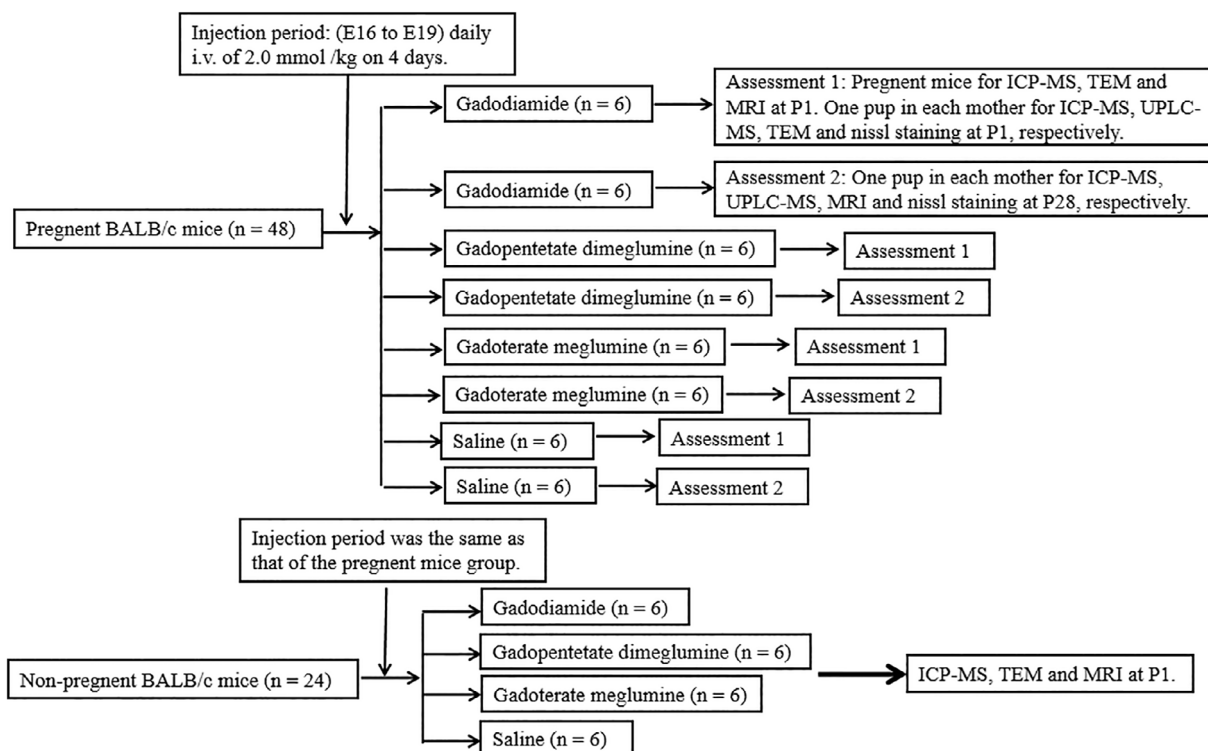


FIGURE 1: Schematic of the study design, including all regimens.

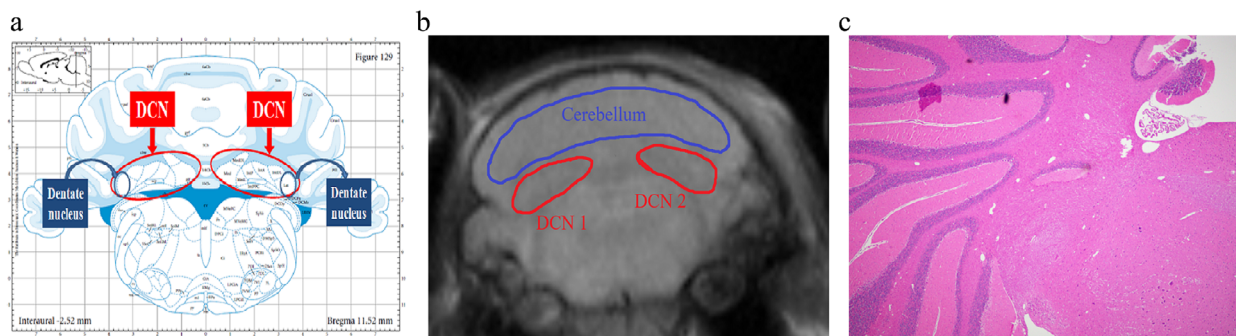


FIGURE 2: (a) Anatomy of mouse brain: localization of the deep cerebellar nuclei (DCN) and dentate nucleus. Extracted from Paxinos and Watson¹¹ with permission. (b) Regions of interest (ROIs) positioning for quantitative analysis. (c) Hematoxylin–eosin staining was used to show the anatomy of the DCN (original magnification, $\times 100$).

was mineralized by microwave heating at 160 °C for 40 min. The microwave laboratory station (MicroSynth; Milestone, Bergamo, Italy) was equipped with an optical fiber temperature control and an HPR-1000/6 M six-position high-pressure reactor. 2) After mineralization, the volume of each sample was brought to 2 mL with ultrapure water and the samples (including pregnant mice, nonpregnant mice, and pup mice) were analyzed by ICP-MS. Calibration curves of 0.005–0.1 $\mu\text{g/mL}$ were obtained using three Gd absorption standard solutions (Sigma Aldrich, Milan, Italy).

At the end of the clearance period, the mice were euthanized with an overdose of sodium pentobarbital anesthesia. Subsequently, the heart was exposed and perfused with 0.9% saline solution to remove excess blood from the brain. The

whole brain was carefully separated and dissected using the mouse brain matrix. Samples of the olfactory bulb, DCN, cerebellum, frontal cortex, hippocampus, and pons were extracted according to the anatomical atlas of the mouse brain.¹²

Brain samples were weighed and sealed in quartz tubes, immersed in 1.5 mL of concentrated nitric acid, and subjected to digestion in a microwave digester for 85 minutes. Each sample was then transferred to a polypropylene tube and diluted to 10 mL with ultra-purified water. Subsequently, ICP-MS (7700x; Agilent Technologies, Santa Clara, California; with an internal standard of indium 115) was used to measure accumulation of the 158 Gd isotope in each sample. The response of the Gd concentration was monitored using

the standard curve of inorganic Gd (0.1–50 $\mu\text{g/L}$) and expressed as nmol of Gd per gram of wet tissue weight.

UPLC-MS Analysis

UPLC-MS was performed for the separation and quantification of intact GBCAs using an Acquity Hclass UPLC system coupled to an Acquity QDa detector. An Acquity UPLC ethylene bridged hybrid hydrophilic interaction liquid chromatographic column ($2.1 \times 3 \times 100$ mm; 1.7 mm particle size) with a VanGuard precolumn was used for isocratic elution with mobile phase A (ammonium formate, 12.5 mM; formic acid, 12.5 mM; 3.75 pH) set at 76% and mobile phase B (acetonitrile) set at 24%. The flow rate was 0.6 mL/min and the total HPLC-MS analysis time was 5 minutes per sample. The column was kept at 40 °C. The conditions of instrumental MS were as follows: capillary voltage, 0.8 kV; cone voltage, 20 V; source temperature, 120 °C; and probe temperature, 600 °C.^{13,14} Establishment of this method involved acquisition of the calibration curves by adding an aliquot of an appropriate internal standard to the brain homogenate at a final concentration of 0.5–10 μM and aliquots of the Gd complexes to be analyzed in the same concentration range. In order to quantify the amount of intact Gd complexes in brain samples, 0.25 nmol of the internal standard (i.e. the selected thulium complex) was added to the brain homogenate. The selected ion monitoring chromatographic peaks of the intact Gd complexes were integrated with the corresponding peaks of the internal standard.

Transmission Electron Microscopy

Brains from pregnant, nonpregnant, and pup mice were separated and washed with cold saline and the DCN were separated on ice as soon as possible. Subsequently, 1 mm³ samples were collected and fixed with 2.5% glutaraldehyde at 4 °C. Samples were rinsed in 0.1 mol/L Na-cacodylate buffer (pH = 7.4) three times, fixed in 1% osmic acid for 2 hours, and washed with saline. Samples were then dehydrated by gradient ethanol and gradient acetone, immersed in Epon812 epoxy resin overnight, dried, and polymerized in an oven at 70 °C for 24 hours. In the next step, ultrathin brain slices (0.1 μm) were cut, stained with 2% lead citrate, and mounted on copper grids. The ultrastructure was observed by TEM (YL, with over 10 years of experience). Energy-dispersive X-ray spectroscopy (EDX) was used to analyze the elemental composition of the observed spots.

Histological Observations

After the pup mice were euthanized at P1 and P28, their brains were removed and fixed in 4% buffered paraformaldehyde for 72 hours. Samples were then dehydrated, embedded in paraffin, cut into 5 μm sections, and stained with hematoxylin and eosin (H&E) and Nissl staining. The number of normal cells was counted under a microscope (Leica, Leica

DM2700 P, Germany) by Haoran Zhang with over 10 years of experience. Histological evaluation of brain injury was performed, including observation of neuronal cell degeneration and obvious necrosis (DS, with over 10 years of experience). They were blinded to the treatment groups. The results were analyzed using ImageJ software.

Statistical Analysis

All data were analyzed using IBM SPSS17.0 or GraphPad Prism 8 software and expressed as the mean \pm standard deviation. An unpaired *t*-test was used to evaluate differences in mean Gd concentrations between groups. Continuous data were analyzed with a one-way analysis of variance (ANOVA) followed by Fisher's least significance difference test between multiple groups. The Mann–Whitney test was used for non-parametric comparisons between the two groups. $P < 0.05$ was considered to be statistically significant.

Results

Animals

All mice successfully completed the study without any adverse health monitoring reports. There were no significant differences in weight about the two groups (48 pregnant BALB/c mice: mean weight 17.5 ± 3.3 g; 24 nonpregnant female mice: mean weight 14.3 ± 1.2 g) during the treatment period and after dosing.

Gd Retention in the Brains of Pregnant and Nonpregnant Mice

Compared with the gadoterate meglumine group, retention of Gd in the DCN and olfactory bulb of maternal brains was significantly higher in the gadopentetate dimeglumine and gadodiamide groups at P1 (0.94 ± 0.14 nmol/g vs. 5.35 ± 0.77 nmol/g and 10.35 ± 2.16 nmol/g for gadopentetate dimeglumine and gadodiamide, respectively) (Fig. 3d). The same significant results were found at nonpregnant mice (1.37 ± 0.24 nmol/g vs. 8.86 ± 1.98 nmol/g and 18.74 ± 3.65 nmol/g for gadopentetate dimeglumine and gadodiamide, respectively). Also, in the area of olfactory bulb, cerebellum, frontal cortex, hippocampus, and pons, retention of Gd in the pregnant mice of gadoterate meglumine group was significantly lower than the gadodiamide and gadopentetate dimeglumine groups (Fig. 3d). Retention of Gd in the olfactory bulb, DCN, cerebellum, frontal cortex, hippocampus, and pons of pregnant mice in the gadodiamide groups was significantly lower than that of nonpregnant mice (14.57 ± 2.37 nmol/g vs. 21.81 ± 3.53 nmol/g; 10.35 ± 2.16 nmol/g vs. 18.74 ± 3.65 nmol/g; 9.41 ± 2.38 nmol/g vs. 16.31 ± 2.66 nmol/g; 8.65 ± 1.73 nmol/g vs. 14.04 ± 1.92 nmol/g; 8.23 ± 1.66 nmol/g vs. 12.62 ± 2.94 nmol/g; and 8.02 ± 1.76 nmol/g vs. 12.09 ± 1.85 nmol/g). In the gadopentetate dimeglumine group, retention of Gd in the six brain areas of pregnant mice was significantly lower than nonpregnant mice, too (Fig. 3a–c). In the gadoterate meglumine group,

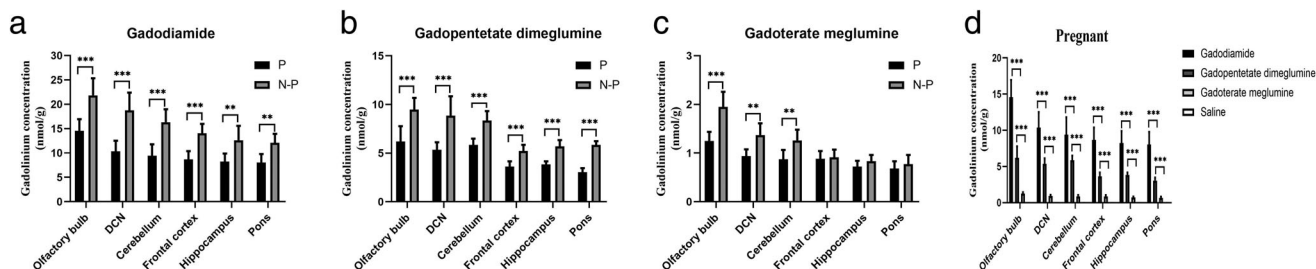


FIGURE 3: (a) Comparison of Gd retention in pregnant and nonpregnant mice brains at postnatal day 1 day after administration of gadodiamide. (b) Comparison of Gd retention in pregnant and nonpregnant mice brains at postnatal day 1 after administration of gadopentetate dimeglumine. (c) Comparison of Gd retention in pregnant and nonpregnant mice brains at postnatal day 1 after administration of gadoterate meglumine. (d) Comparison of Gd retention in pregnant mice brains at postnatal day 1 after administration of gadodiamide, gadopentetate dimeglumine, and gadoterate meglumine. * $P < 0.05$, ** $P < 0.01$, *** $P < 0.001$.

the significant differences in Gd retention between pregnant and nonpregnant mice were also observed in the olfactory bulb, DCN, and cerebellum (Fig. 3a–c). The olfactory bulb and DCN showed the highest Gd retention in the group of gadodiamide (olfactory bulb: 14.57 ± 2.37 nmol/g and 21.81 ± 3.53 nmol/g for pregnant and nonpregnant mice at P1; DCN: 10.35 ± 2.16 nmol/g and 18.74 ± 3.65 nmol/g for pregnant and nonpregnant mice at P1). Among the other two GBCAs groups, olfactory bulb and DCN also showed the highest Gd retention (Fig. 3a–c).

Gd Retention in Pup Brains

By ICP-MS, we found that compared with the gadoterate meglumine group, retention of Gd in the DCN and olfactory bulb of pups was significantly higher in the gadopentetate dimeglumine and gadodiamide groups at P1 (0.21 ± 0.09 nmol/g vs. 2.21 ± 1.34 nmol/g and 6.15 ± 3.21 nmol/g for gadopentetate dimeglumine and gadodiamide, respectively) (Fig 4a). The same significant results were found at P28 in the area of DCN (0.08 ± 0.03 nmol/g vs. 0.78 ± 0.34 nmol/g and 1.98 ± 0.76 nmol/g for gadopentetate dimeglumine and gadodiamide, respectively) (Fig 4b). Also, in the area of olfactory bulb, DCN, cerebellum, frontal cortex, hippocampus, and pons, retention of Gd in the pups (P1 and P28) of gadoterate meglumine group was significantly lower than the gadodiamide and

gadopentetate dimeglumine groups (Fig. 4). The olfactory bulb and DCN showed the highest Gd retention in the group of gadodiamide (olfactory bulb: 7.32 ± 3.32 nmol/g and 2.11 ± 0.87 nmol/g for pup mice at P1 and P28; DCN: 6.15 ± 3.21 nmol/g and 1.98 ± 0.76 nmol/g for pup mice at P1 and P28). Among the other two GBCAs groups, olfactory bulb and DCN also showed the highest Gd retention (Fig. 4).

Determination of Intact GBCAs by UPLC-MS in Pups at P28

Figure 5 reports the mean percentages of intact Gd complexes in pups at P28 determined by UPLC-MS analysis of soluble extracts in mice treated with gadodiamide, gadopentetate dimeglumine, or gadoterate meglumine. After intravenous injection of gadoterate meglumine, the total amount of recovered Gd in brain tissue were close to the amount of intact Gd. In contrast, in the corresponding experiments with gadodiamide, only $30.5\% \pm 7.1\%$, $19.5\% \pm 9.5\%$, $18.2\% \pm 10.6\%$, $13.6\% \pm 8.1\%$, $27.1\% \pm 12.7\%$, and $15.6\% \pm 7.7\%$ of the recovered amount corresponded to the intact complex in the olfactory bulb, DCN, cerebellum, frontal cortex, hippocampus, and pons, respectively. In the gadodiamide group, the intact Gd complexes in pups' DCN were significantly lower than those in the gadopentetate dimeglumine and gadoterate meglumine

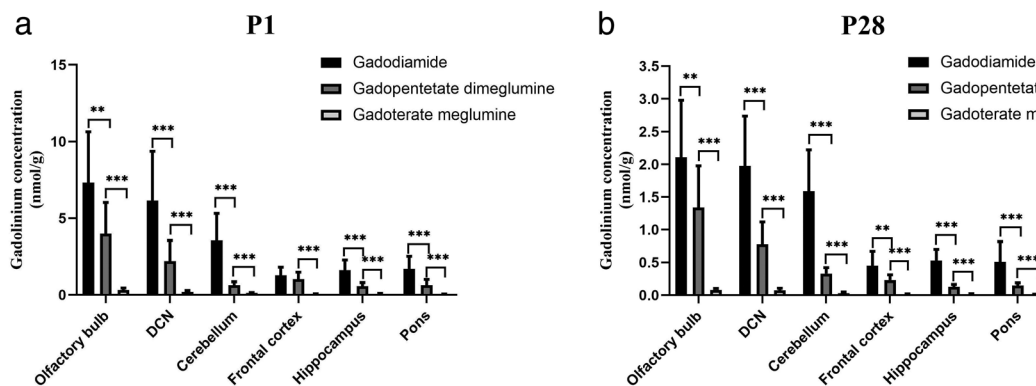


FIGURE 4: (a) Comparison of Gd retention in pup mice brains at postnatal day 1 after administration of gadodiamide, gadopentetate dimeglumine, and gadoterate meglumine. (b) Comparison of Gd retention in pup mice brains at postnatal day 28 after administration of gadodiamide, gadopentetate dimeglumine, and gadoterate meglumine. * $P < 0.05$, ** $P < 0.01$, *** $P < 0.001$.

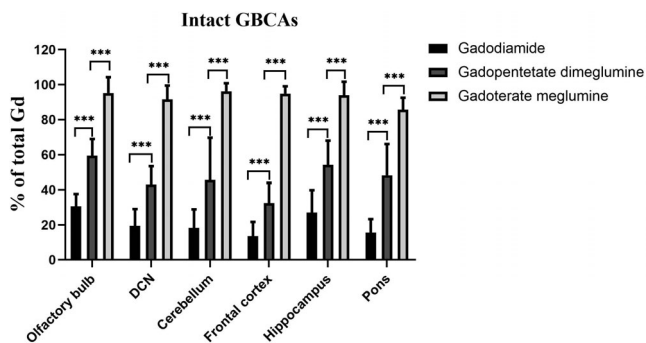


FIGURE 5: Comparison of intact gadolinium-based contrast agents (GBCAs) retention in pup mice brains at postnatal day 28 after administration of gadodiamide, gadopentetate dimeglumine, and gadoterate meglumine. **P* < 0.05, ***P* < 0.01, ****P* < 0.001.

groups (19.5% ± 9.5%, 43.1% ± 10.3%, and 91.6% ± 7.9% for gadodiamide, gadopentetate dimeglumine, and gadoterate meglumine group, respectively). We found the same significant results in the other five regions.

Magnetic Resonance Image

As shown, coronal MR images transecting the placenta and uterus in a pregnant mice, which was injected with gadodiamide via the tail vein for 4 consecutive days (E16–E19) at a dose of 2.0 mmol/kg on E19 (Fig. 6). At the last GBCAs injection, there was no significant difference in T₁ signal between pregnant and nonpregnant mice for the area of the DCN (*P* = 0.221). No difference in enhancement in T₁ signal was observed in the area of the DCN between pregnant mice injected with GBCAs and saline (*P* = 0.316). Among the pup groups, no significant difference was found in the T₁ signal intensity ratio of the DCN (*P* = 0.554) (Fig. 7).

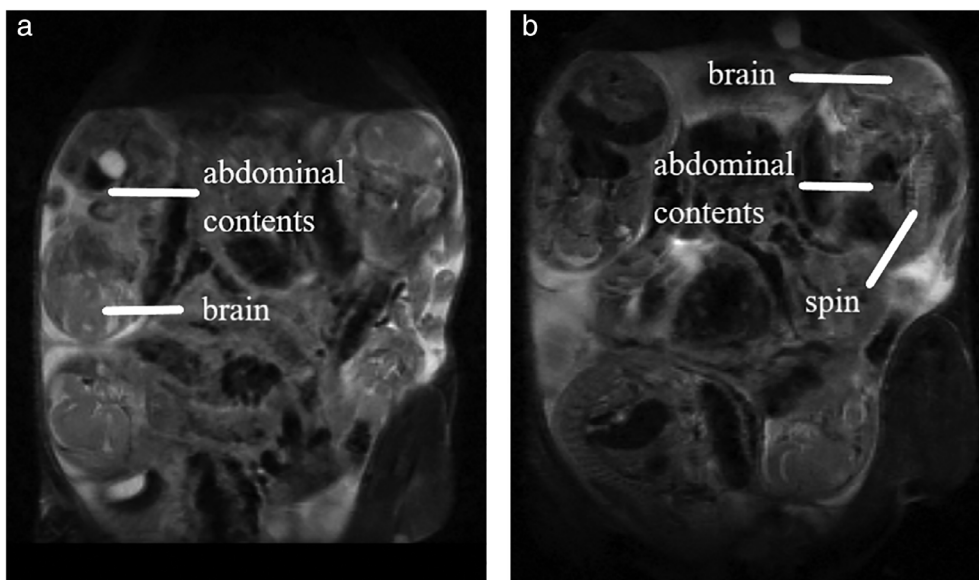


FIGURE 6: Coronal T₂-weighted MRI images transecting the placenta and uterus in two pregnant mice on E19. The brain, spine, and abdominal contents are outlined in white arrows.

TEM Analysis of Gd Deposits in Brains

In both the gadodiamide, gadopentetate dimeglumine and gadoterate meglumine groups, electron-dense granules were observed by TEM in the olfactory bulb of pregnant mice, nonpregnant mice, and pups at P1. These electron-dense Gd deposits were mainly in the endothelial walls of capillaries (Fig. 8).

Histologic Toxicology Findings

According to the anatomical atlas of the mice brain, hematoxylin–eosin staining was used to show the DCN. Nissl staining was used to assess the DCN of the pups. At P1 and P28, the pups of the four groups were killed (three sections per animal, six mice per group) and examined (Fig. 9). All results were within the normal limits compared with saline group. There was no statistical difference between the four groups about the number of normal cells, observation of neuronal cell degeneration, and obvious necrosis (*P* = 0.415).

Discussion

In the present study, we demonstrated that the retention rate of Gd in the brains of pregnant mice was generally lower than that in nonpregnant mice. Furthermore, the Gd retention rate after gadodiamide administration was always higher than that of gadoterate meglumine administration in both mothers and pups. We suspect that the difference in Gd retention between pregnant and nonpregnant mice may be due to the physiological increase in the glomerular filtration rate and renal plasma flow. We also observed retention of Gd in the brains of the pups after maternal administration of GBCAs. This finding suggests that fetal tissue may be an additional, unfortunate way of Gd elimination from the mother. These

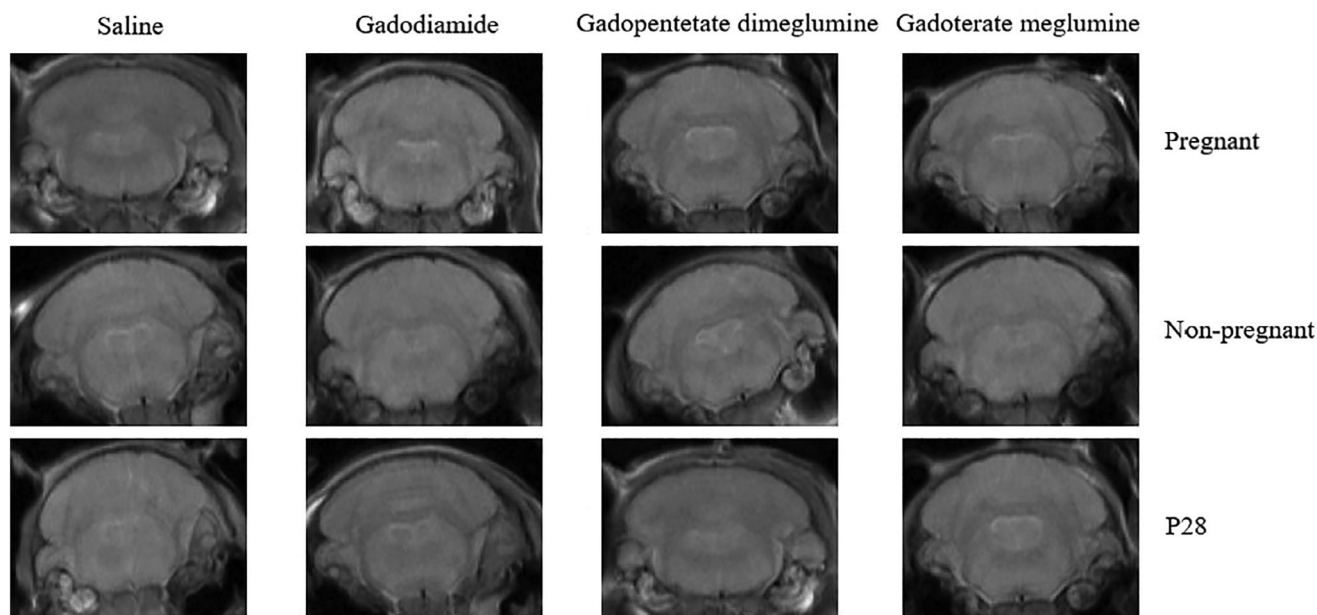


FIGURE 7: Representative T₁-weighted MR images of the deep cerebellar nuclei (DCN) in pup mice at postnatal day 28, pregnant and non-pregnant mice at postnatal day 1 after injections of saline, gadodiamide, gadopentetate dimeglumine, and gadoterate meglumine. There were no increased signal intensities on the T₁-weighted MR images of the DCN among all groups.

results may partially explain Khurana's report in which the symptoms of nephrogenic systemic fibrosis (NSF) improved after pregnancy.¹⁵ The retention rate of Gd in the pups of mothers administered GBCAs during pregnancy varied with the type of GBCAs. Gd was found in the brains of both mothers and pups exposed to GBCAs. This finding is consistent with previous clinical and laboratory reports.^{16–18} The organ-to-muscle ratio of Gd retention in the brains of pups was higher than that in the maternal brains. This result may be due to the immaturity of the fetal blood–brain barrier (BBB).¹⁹ However, even in the adult BBB, Gd entered brain tissue and was retained 28 days after the last injection.

At present, the mechanism of Gd uptake and retention in the brain remains unclear. One hypothesis is dechelation caused by transmetalation and subsequent interaction with organic macromolecules, considering that high T₁-weighted signals are mainly in the dentate nucleus and thalamus.^{20,21} Other metal ions, such as iron and calcium, also tend to show relatively high concentrations. The absorption and accumulation of Gd may be mediated by biological mechanisms, such as metal transporters. There are two potential ways for GBCAs to penetrate and clear the brain, namely through the BBB and the glymphatic system.^{22,23} Taoka and Naganawa found that, when the lymphatic system tends to be active, animals administered GBCAs under anesthesia or during sleep show a low retention rate of Gd.²⁴ This indicates that the glymphatic system may be involved in the retention of Gd in the brain. In pregnant mice, nonpregnant mice, and pups, the Gd concentration in the olfactory bulb was higher than that in most other parts of the brain. This finding is consistent with a previous study by Kartamihardja et al in

which the Gd concentration in the olfactory bulb of the gadodiamide group was the highest.²⁵ The olfactory bulb is proposed to be an important part of the normal functioning of the glymphatic system. The acetylcholine system is a recently described paravascular pathway for cerebrospinal fluid (CSF) and interstitial fluid exchange in the brain. It can remove waste proteins and metabolites. Recent studies have shown that the glymphatic system is a potential pathway for GBCAs to enter the brain.²⁶

After injection of GBCAs into the subarachnoid space of the cisterna magna, GBCAs have been shown to rapidly enter the brain parenchyma, especially the olfactory bulb and cerebellum, along the paravascular pathway from the basilar artery to the olfactory artery.²⁷ In contrast, CSF flows from the subarachnoid space through the olfactory bulb to the peripheral lymphatic system along the cranial and spinal nerves.²⁸ The olfactory pathway is considered to be one of the most important efflux pathways for CSF in the brain, which may explain the higher concentration of Gd in the olfactory bulb.²⁹ Increasing evidence has shown that the dentate nucleus and globus pallidus are two targets for the accumulation of metals such as copper and zinc.^{30,31} In addition, it has been confirmed that divalent metals in the dentate nucleus and globus pallidus are transferred when chronically exposed to manganese and lanthanum.³² Both lanthanum and Gd are lanthanides and have similar properties. Therefore, Gd may also be involved in the transfer of divalent metals in the dentate nucleus and globus pallidus and be deposited in these brain regions.

The activity of Ca²⁺-adenosine triphosphatase in the brain is inhibited in rats exposed to lanthanum, and

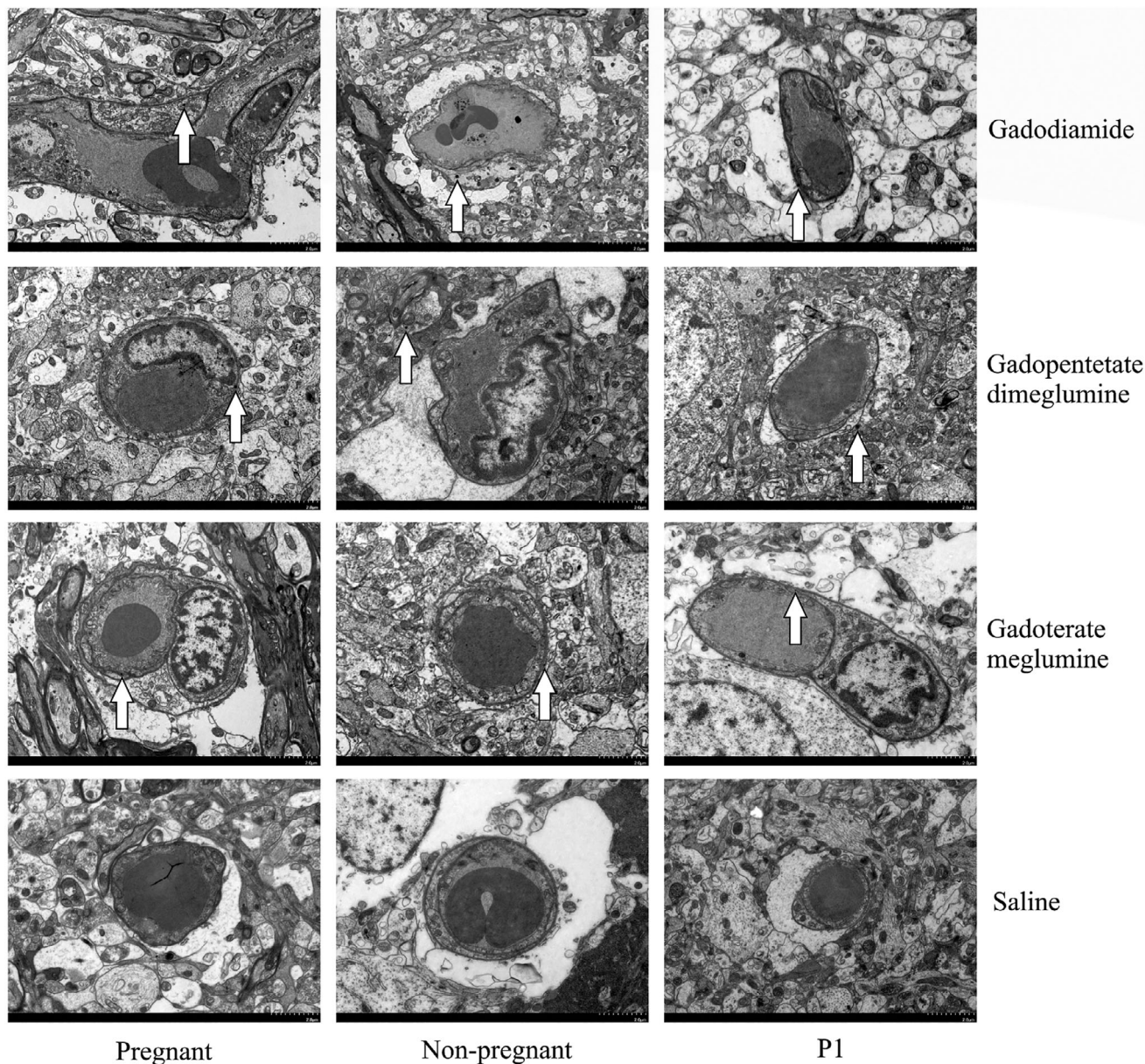


FIGURE 8: Localization of Gd deposits in the deep cerebellar nuclei (DCN) of pregnant, nonpregnant, and pup mice at postnatal day 1 by transmission electron microscopy. Electron-dense granules are indicated by white arrows.

homeostasis of trace elements, enzymes, and neurotransmitter systems is disturbed.³² However, to date, there is no evidence demonstrating that lanthanum ions have the same metabolism effects as dechelated Gd. Furthermore, there is no evidence of neurotoxicological consequences in patients and animals with Gd retention. Dechelation may occur during the formation of a stable species, where Gd is secured and inactivated.

Consistent with previous studies, our study showed that the amount of retained Gd in mice exposed to linear neutral GBCAs Gd was much higher than that in animals exposed to macrocyclic neutral GBCAs gadoteridol.^{33–37} However, in all brain regions in mice treated with gadoterate meglumine, the amount of retained total Gd was significantly higher than that

in the control group. After administration of gadoterate meglumine, the total amount of Gd in the brain corresponded entirely to the intact gadoteridol. In contrast, after administration of gadodiamide, only a small amount of intact complex was found. This indicates that a large fraction of the administered gadodiamide is converted into insoluble species. This finding is consistent with an earlier study by McDonald et al that reported Gd-containing deposits observed by TEM obtained from postmortem biopsy of human brain tissue.³⁸ These results are also consistent with a recent study by Frenzel et al that reported the chemical form of residual Gd in the brain.³⁹ They found that Gd was only present in soluble parts of the brain tissue and only as low-molecular-weight molecules in animals treated with macrocyclic GBCAs.

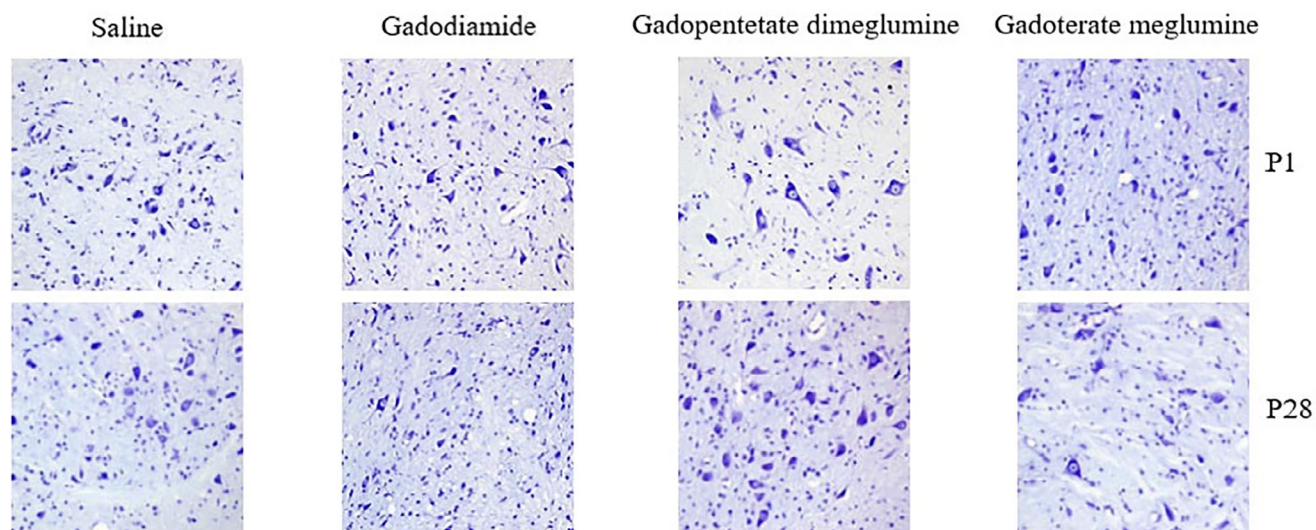


FIGURE 9: No histopathologic abnormalities were observed in pup mice at postnatal days 1 and 28 after administration of gadodiamide, gadopentetate dimeglumine, and gadoterate meglumine. High-power representative photomicrographs (Nissl staining; original magnification, $\times 200$) of the DCN (lower expanded panels) of mice treated with saline, gadodiamide, gadopentetate dimeglumine, and gadoterate meglumine are shown.

However, Gd was highly present in insoluble tissues in mice treated with linear GBCAs. In this study, the low-molecular-weight molecules found in the soluble fraction corresponded to the intact Gd complex. The chemical form of Gd-containing insoluble species has not yet been determined. However, it is reasonable to assume that any solid form of Gd makes little contribution to the high signal intensity on T_1 -weighted MR images as water access to paramagnetic centers in solids is limited. In our experiments, the separation method did not exclude the part of the membrane or protein-bound Gd. Gianolio et al also found that the sum of insoluble Gd species (53%) and intact GBCAs (18%) were found in the cerebellar tissue of the animals treated with Gd.⁴⁰ This finding is relevant to the high signal detected on the T_1 -weighted image of the cerebellum area, which showed an estimated signal enhancement of approximately 10%. This is not dissimilar from reports for analogous experimental setups.⁴¹

In general, the results reported in the current paper are consistent with the view that GBCAs begin their journey after crossing the BBB or CSF barrier. This journey seems to be strongly influenced by kinetic and thermodynamic stability and the composition of the tissue area experienced by the GBCAs. The stability of gadodiamide is not as good as that of gadoterate meglumine. Based on the available data, we cannot say much about the chemical form of the insoluble and highly relaxed soluble Gd-containing species. We can only determine the amount of intact GBCAs in the total Gd. We cannot say whether deacetylation corresponds to complete separation between gadodiamide ligands and Gd ions or if there is a ternary complex that still contains ligands associated with the biomolecules. The potential role of sialic acid-containing macromolecules is reasonable because there are

many of these and similar molecules on the surface of glial cells. It is very important to carefully evaluate the potential risks of Gd retention in the brain and the significant diagnostic benefits of contrast-enhanced MRI. The lack of acute histopathological findings in the brains of our experimental mice is consistent with previous studies, although our study included mice with an extended exposure time of 28 days after birth. Our study also included perfusion fixation to optimize morphological preservation and allow standardized assessment of brain toxicology. This is consistent with the method used in safety toxicology research. We believe that histopathological analysis is very important after acute and chronic exposure. This analysis can eliminate the possibility of acute toxicity and delayed toxicity, which may be obvious only after long-term exposure. The lack of histopathologic findings in the brain is consistent with a lack of in-life sequelae in this study or similar animal studies. In view of the similar placental physiology between humans and mice, we believe that after maternal injection of gadoteridol, there is relatively little retention in human fetal tissues. However, the long-term risks of low-level Gd retention are still unknown. We did not evaluate the effects of Gd retention on the normal development of pups. Intensive observations, including behavioral research, are needed to evaluate the effects of Gd retention on normal development.

Limitations

Our study had several limitations. The glymphatic system is one of the way for GBCAs to penetrate and clear the brain. During sleep or anesthesia, the lymphatic system tends to be active. Animals administered GBCAs under anesthesia or during sleep show a low retention rate of Gd. The limitations of

our study include the assessment of the effect of the pregnant status on Gd retention in the brain only. The potential effects of GBCAs on other organs were not evaluated, such as NSF. Although, the differences between humans and mice on placental physiology may affect the results. We only evaluated the three GBCAs, and other approved and available GBCAs were not included.

Conclusion

This study revealed that intrauterine Gd was retained by placenta in pup mice. The Gd concentrations in the brains were lower for pregnant mice than for nonpregnant mice. In various brain areas in both mother and pup mice, Gd retention was consistently higher for gadoterate meglumine. The olfactory bulb and DCN showed the highest Gd retention. By detecting the intact GBCAs, we found that gadoterate meglumine was more stable than the other two.

Acknowledgments

The authors gratefully appreciate the assistance of Zicheng Huang from the Center for Molecular Imaging and Translational Medicine of Xiamen University for her technical assistance with the MRI procedures. This work was supported by National Natural Science Foundation of China (Grant 82071886) and Scientific Research Foundation for Advanced Talents, Xiang'an Hospital of Xiamen University (No. PM201809170011).

Conflicts of interest

The authors have no potential conflicts of interest to disclose.

References

- Erdene K, Nakajima T, Kameo S, et al. Organ retention of gadolinium in mother and pup mice: Effect of pregnancy and type of gadolinium-based contrast agents. *Jpn J Radiol* 2017;35(10):568-573. <https://doi.org/10.1007/s11604-017-0667-2>.
- ACR Committee on Drugs and Contrast Media. Manual on Contrast Media v10.2 2016 2016 Accessed November 3, 2016. Available from: <https://www.acr.org/quality-safety/resources/contrast-manual>
- ESUR Contrast media safety committee. ESUR Guidelines on Contrast Media, version 9. 2016. Accessed November 3, 2016. Available from: <https://www.esur.org/esur-guidelines/>
- Radbruch A, Richter H, Fingerhut S, et al. Gadolinium deposition in the brain in a large animal model: Comparison of linear and macrocyclic gadolinium-based contrast agents. *Invest Radiol* 2019;54(9):531-536. <https://doi.org/10.1097/RLI.0000000000000575>.
- Kong Y, Zhang S, Wang J, et al. Potential toxicity evaluation and comparison within multiple mice organs after repeat injections of linear versus macrocyclic gadolinium-based contrast agents: A comprehensive and time course study. *Toxicol Lett* 2021;350:152-161. <https://doi.org/10.1016/j.toxlet.2021.07.016>.
- Robert P, Violas X, Grand S, et al. Linear gadolinium-based contrast agents are associated with brain gadolinium retention in healthy rats. *Invest Radiol* 2016;51(2):73-82. <https://doi.org/10.1097/RLI.0000000000000241>.
- Arena F, Bardini P, Blasi F, et al. Gadolinium presence, MRI hyperintensities, and glucose uptake in the hypoperfused rat brain after repeated administrations of gadodiamide. *Neuroradiology* 2019;61(2):163-173. <https://doi.org/10.1007/s00234-018-2120-3>.
- Gianolio E, Bardini P, Arena F, et al. Gadolinium retention in the rat brain: Assessment of the amounts of insoluble gadolinium-containing species and intact gadolinium complexes after repeated Administration of Gadolinium-based Contrast Agents. *Radiology* 2017;285(3):839-849. <https://doi.org/10.1148/radiol.2017162857>.
- Oh KY, Roberts VH, Schabel MC, Grove KL, Woods M, Frias AE. Gadolinium chelate contrast material in pregnancy: Fetal biodistribution in the nonhuman primate. *Radiology* 2015;276(1):110-118. <https://doi.org/10.1148/radiol.15141488>.
- Schabel MC, Parker DL. Uncertainty and bias in contrast concentration measurements using spoiled gradient echo pulse sequences. *Phys Med Biol* 2008;53(9):2345-2373. <https://doi.org/10.1088/0031-9155/53/9/010>.
- Schabel MC, Morrell GR. Uncertainty in T(1) mapping using the variable flip angle method with two flip angles. *Phys Med Biol* 2009;54(1):N1-N8. <https://doi.org/10.1088/0031-9155/54/1/N01>.
- Paxinos G, Watson C. *The rat brain in stereotaxic coordinates*. 6th ed. London, UK: Academic Press; 2007.
- Künemeyer J, Terborg L, Nowak S, et al. Speciation analysis of gadolinium-based MRI contrast agents in blood plasma by hydrophilic interaction chromatography/electrospray mass spectrometry. *Anal Chem* 2008;80(21):8163-8170. <https://doi.org/10.1021/ac801264j>.
- Birka M, Wentker KS, Luschmüller E, et al. Diagnosis of nephrogenic systemic fibrosis by means of elemental bioimaging and speciation analysis. *Anal Chem* 2015;87(6):3321-3328. <https://doi.org/10.1021/ac504488k>.
- Khurana A, Nickel AE, Greene JF, Narayanan M, High WA, Foulks CJ. Successful pregnancy in a hemodialysis patient and marked resolution of her nephrogenic systemic fibrosis. *Am J Kidney Dis* 2008;51(6):e29-e32. <https://doi.org/10.1053/j.ajkd.2007.12.037>.
- Kanda T, Ishii K, Kawaguchi H, Kitajima K, Takenaka D. High signal intensity in the dentate nucleus and globus pallidus on unenhanced T1-weighted MR images: Relationship with increasing cumulative dose of a gadolinium-based contrast material. *Radiology* 2014;270(3):834-841. <https://doi.org/10.1148/radiol.13131669>.
- Kanda T, Fukusato T, Matsuda M, et al. Gadolinium-based contrast agent accumulates in the brain even in subjects without severe renal dysfunction: Evaluation of autopsy brain specimens with inductively coupled plasma mass spectroscopy. *Radiology* 2015;276(1):228-232. <https://doi.org/10.1148/radiol.2015142690>.
- Rowe SK, Rodriguez D, Cohen E, et al. Switching from linear to macrocyclic gadolinium-based contrast agents halts the relative T1-weighted signal increase in deep gray matter of children with brain tumors: A retrospective study. *J Magn Reson Imaging* 2020;51(1):288-295. <https://doi.org/10.1002/jmri.26831>.
- Liebner S, Dijkhuizen RM, Reiss Y, Plate KH, Agalliu D, Constantin G. Functional morphology of the blood-brain barrier in health and disease. *Acta Neuropathol* 2018;135(3):311-336. <https://doi.org/10.1007/s00401-018-1815-1>.
- Ramalho M, Ramalho J, Burke LM, Semelka RC. Gadolinium retention and toxicity-an update. *Adv Chronic Kidney Dis* 2017;24(3):138-146. <https://doi.org/10.1053/j.ackd.2017.03.004>.
- Kanda T, Nakai Y, Oba H, Toyoda K, Kitajima K, Furui S. Gadolinium deposition in the brain. *Magn Reson Imaging* 2016;34(10):1346-1350. <https://doi.org/10.1016/j.mri.2016.08.024>.
- Naganawa S, Nakane T, Kawai H, Taoka T. Gd-based contrast enhancement of the perivascular spaces in the basal ganglia. *Magn Reson Med Sci* 2017;16(1):61-65. <https://doi.org/10.2463/mrms.mp.2016-0039>.
- Prybylski JP, Maxwell E, Coste Sanchez C, Jay M. Gadolinium deposition in the brain: Lessons learned from other metals known to cross the blood-brain barrier. *Magn Reson Imaging* 2016;34(10):1366-1372. <https://doi.org/10.1016/j.mri.2016.08.018>.
- Taoka T, Naganawa S. Gadolinium-based contrast media, cerebrospinal fluid and the glymphatic system: Possible mechanisms for the deposition of gadolinium in the brain. *Magn Reson Med Sci* 2018;17(2):111-119. <https://doi.org/10.2463/mrms.rev.2017-0116>.

25. Kartamihardja AA, Nakajima T, Kameo S, Koyama H, Tsushima Y. Distribution and clearance of retained gadolinium in the brain: Differences between linear and macrocyclic gadolinium based contrast agents in a mouse model. *Br J Radiol* 2016;89(1066):20160509. <https://doi.org/10.1259/bjr.20160509>.
26. Jost G, Frenzel T, Lohrke J, Lenhard DC, Naganawa S, Pietsch H. Penetration and distribution of gadolinium-based contrast agents into the cerebrospinal fluid in healthy rats: A potential pathway of entry into the brain tissue. *Eur Radiol* 2017;27(7):2877-2885. <https://doi.org/10.1007/s00330-016-4654-2>.
27. Iliff JJ, Lee H, Yu M, et al. Brain-wide pathway for waste clearance captured by contrast-enhanced MRI. *J Clin Invest* 2013;123(3):1299-1309. <https://doi.org/10.1172/JCI67677>.
28. Murtha LA, Yang Q, Parsons MW, et al. Cerebrospinal fluid is drained primarily via the spinal canal and olfactory route in young and aged spontaneously hypertensive rats. *Fluids Barriers CNS* 2014;11:12. <https://doi.org/10.1186/2045-8118-11-12>.
29. Kanda T, Osawa M, Oba H, et al. High signal intensity in dentate nucleus on unenhanced T1-weighted MR images: Association with linear versus macrocyclic gadolinium chelate administration. *Radiology* 2015;275(3):803-809. <https://doi.org/10.1148/radiol.14140364>.
30. Popescu BF, Robinson CA, Rajput A, Rajput AH, Harder SL, Nichol H. Iron, copper, and zinc distribution of the cerebellum. *Cerebellum (London, England)* 2009;8(2):74-79. <https://doi.org/10.1007/s12311-008-0091-3>.
31. Erikson KM, Syversen T, Steinnes E, Aschner M. Globus pallidus: A target brain region for divalent metal accumulation associated with dietary iron deficiency. *J Nutr Biochem* 2004;15(6):335-341. <https://doi.org/10.1016/j.jnutbio.2003.12.006>.
32. Feng L, Xiao H, He X, et al. Neurotoxicological consequence of long-term exposure to lanthanum. *Toxicol Lett* 2006;165(2):112-120. <https://doi.org/10.1016/j.toxlet.2006.02.003>.
33. Wang ST, Hua ZX, Fan DX, Zhang X, Ren K. Gadolinium retention and clearance in the diabetic brain after administrations of gadodiamide, gadopentetate dimeglumine, and gadoterate meglumine in a rat model. *BioMed Research International*, 2019;3901907. <https://doi.org/10.1155/2019/3901907>
34. Radbruch A, Richter H, Bücken P, et al. Is small fiber neuropathy induced by gadolinium-based contrast agents? *Invest Radiol* 2020; 55(8):473-480. <https://doi.org/10.1097/RLI.0000000000000677>.
35. Erdoğan MA, Apaydin M, Armagan G, Taskiran D. Evaluation of toxicity of gadolinium-based contrast agents on neuronal cells. *Acta Radiol (Stockholm, Sweden: 1987)* 2021;62(2):206-214. <https://doi.org/10.1177/0284185120920801>.
36. Costelloe CM, Amini B, Madewell JE. Risks and benefits of gadolinium-based contrast-enhanced MRI. *Semin Ultrasound CT MR* 2020;41(2): 170-182. <https://doi.org/10.1053/j.sult.2019.12.005>.
37. Kiviniemi A, Gardberg M, Ek P, Frantzén J, Bobacka J, Minn H. Gadolinium retention in gliomas and adjacent normal brain tissue: Association with tumor contrast enhancement and linear/macrocytic agents. *Neuroradiology* 2019;61(5):535-544. <https://doi.org/10.1007/s00234-019-02172-6>.
38. McDonald RJ, McDonald JS, Kallmes DF, et al. Intracranial gadolinium deposition after contrast-enhanced MR imaging. *Radiology* 2015; 275(3):772-782. <https://doi.org/10.1148/radiol.15150025>.
39. Frenzel T, Apte C, Jost G, Schöckel L, Lohrke J, Pietsch H. Quantification and assessment of the chemical form of residual gadolinium in the brain after repeated Administration of Gadolinium-Based Contrast Agents: Comparative study in rats. *Invest Radiol* 2017;52(7):396-404. <https://doi.org/10.1097/RLI.0000000000000352>.
40. Gianolio E, Cabella C, Colombo Serra S, et al. B25716/1: A novel albumin-binding Gd-AAZTA MRI contrast agent with improved properties in tumor imaging. *J Biol Inorg Chem* 2014;19(4-5):715-726. <https://doi.org/10.1007/s00775-014-1111-z>.
41. Kartamihardja AA, Nakajima T, Kameo S, Koyama H, Tsushima Y. Impact of impaired renal function on gadolinium retention after Administration of Gadolinium-Based Contrast Agents in a mouse model. *Invest Radiol* 2016;51(10):655-660. <https://doi.org/10.1097/RLI.0000000000000295>.